Molecular Therapy
Oncolytics
Original Article

The pivotal regulatory factor circBRWD1 inhibits arsenic exposure-induced lung cancer occurrence by binding mRNA and regulating its stability

Xiaofei Li,[1,2,3,5] Sixian Chen,[1,2,3,5] Xin Wang,[4,5] Ruirui Zhang,[1,2,3] Jialei Yang,[2] Haotian Xu,[1,2,3] Wanting He,[2] Mingshuang Lai,[2] Shuilian Wu,[4] and Aruo Nan[1,2,3,4]

[1]Department of Toxicology, School of Public Health, Guangxi Medical University, Guangxi Colleges and Universities Key Laboratory of Prevention and Control of Highly Prevalent Diseases, Nanning 530021, China; [2]Guangxi Colleges and Universities Key Laboratory of Prevention and Control of Highly Prevalent Diseases, Guangxi Medical University, Nanning 530021, China; [3]Guangxi Key Laboratory of Environment and Health Research, Guangxi Medical University, Nanning 530021, China; [4]Zhejiang Provincial Key Laboratory for Technology and Application of Model Organisms, Key Laboratory of Laboratory Medicine, Ministry of Education, School of Laboratory Medicine and Life Sciences, Wenzhou Medical University, Wenzhou 325035, China

Multiple studies have indicated that circular RNAs (circRNAs) play a regulatory role in different stages of tumors by interacting with various molecules. With continuous in-depth research on the biological functions of circRNAs, increasing evidence has shown that circRNAs play important roles in carcinogenesis caused by environmental pollutants. However, the function and mechanism of circRNAs in arsenic exposure-induced lung cancer occurrence have not been reported. In this study, RNA sequencing and qPCR assays revealed that the expression of circBRWD1 was decreased in BEAS-2B-As cells and multiple lung cancer cell lines. Silencing circBRWD1 promoted cell viability and proliferation, inhibited cell apoptosis, and accelerated the G0/G1 phase transition in BEAS-2B-As cells; however, these functions were abrogated by circBRWD1 overexpression. Mechanistically, under arsenic exposure, expression of decreased circBRWD1 led to enhanced stability of the mRNA to which it directly binds (c-JUN, c-MYC, and CDK6 mRNA), increasing its expression. This mechanism promotes the malignant transformation of lung cells and ultimately leads to lung cancer. Our findings thus reveal the molecular mechanism of arsenic carcinogenesis.

INTRODUCTION

In 2020, the authoritative cancer report of the International Agency for Research on Cancer (IARC) showed that the mortality and morbidity of lung cancer in the world rank first and second, respectively, among all malignant tumors, while death from lung cancer and new lung cancer cases rank first among all malignant tumors in China, seriously endangering human life and health.[1] However, to date, the pathogenesis of lung cancer is still unclear, with many factors playing specific roles in the pathogenesis of lung cancer. Hence, lung cancer is the comprehensive result of many factors. In addition to smoking, family cancer history, respiratory diseases, and other factors, environmental chemical carcinogen exposure is an important factor in lung cancer occurrence.

Arsenic is one of the most common environmental pollutants, occurring naturally in rocks, soil, and water. Arsenic is also a known human carcinogen that exists in nature and is toxic to humans, leading to various adverse effects and diseases.[2] In contaminated environments, arsenic contributes to harmful effects on an increasing number of people.[3] Exposure to arsenic causes cardiovascular disease,[4] diabetes mellitus,[5] and malignancies, such as lung cancer[6] and bladder cancer.[7] Chronic exposure to arsenic might result in oxidative DNA damage[8] and epigenetic changes such as DNA methylation.[9] Arsenic induces carcinogenesis by regulating hallmark signaling pathways, such as cell proliferation, apoptosis, and cell-cycle pathways.[10] Growing evidence shows that arsenic not only changes genomic stability but also promotes transcriptional dysregulation by affecting microRNAs (miRNAs)[11] and long noncoding RNAs.[12] With a broader understanding of next-generation sequencing, recent studies have demonstrated that circular RNAs (circRNAs) might function as mediators of pathogenic arsenic-related signaling pathways in carcinogenesis.[13]

circRNAs, originating from protein-coding genes, constitute a class of endogenous regulatory RNAs. The exonic sequences generated by back splicing form a loop structure with joined 5′ and 3′ ends.[14] circRNAs are involved in diverse biological functions, such as the cell cycle, cell differentiation, and apoptosis.[15] circRNAs can function as a "sponge" that binds to RNA-binding proteins and ribonucleoprotein complexes. This sponging action is altered in a pathological environment and during disease development, as well as during cancer cell migration and invasion. circRNAs are involved in epithelial-mesenchymal transition

Received 6 January 2022; accepted 18 August 2022;
https://doi.org/10.1016/j.omto.2022.08.006.

[5]These authors contributed equally

Correspondence: Aruo Nan, PhD, Department of Toxicology, School of Public Health, Guangxi Medical University, Guangxi Colleges and Universities Key Laboratory of Prevention and Control of Highly Prevalent Diseases, Nanning 530021, China.
E-mail: nanaruo@163.com

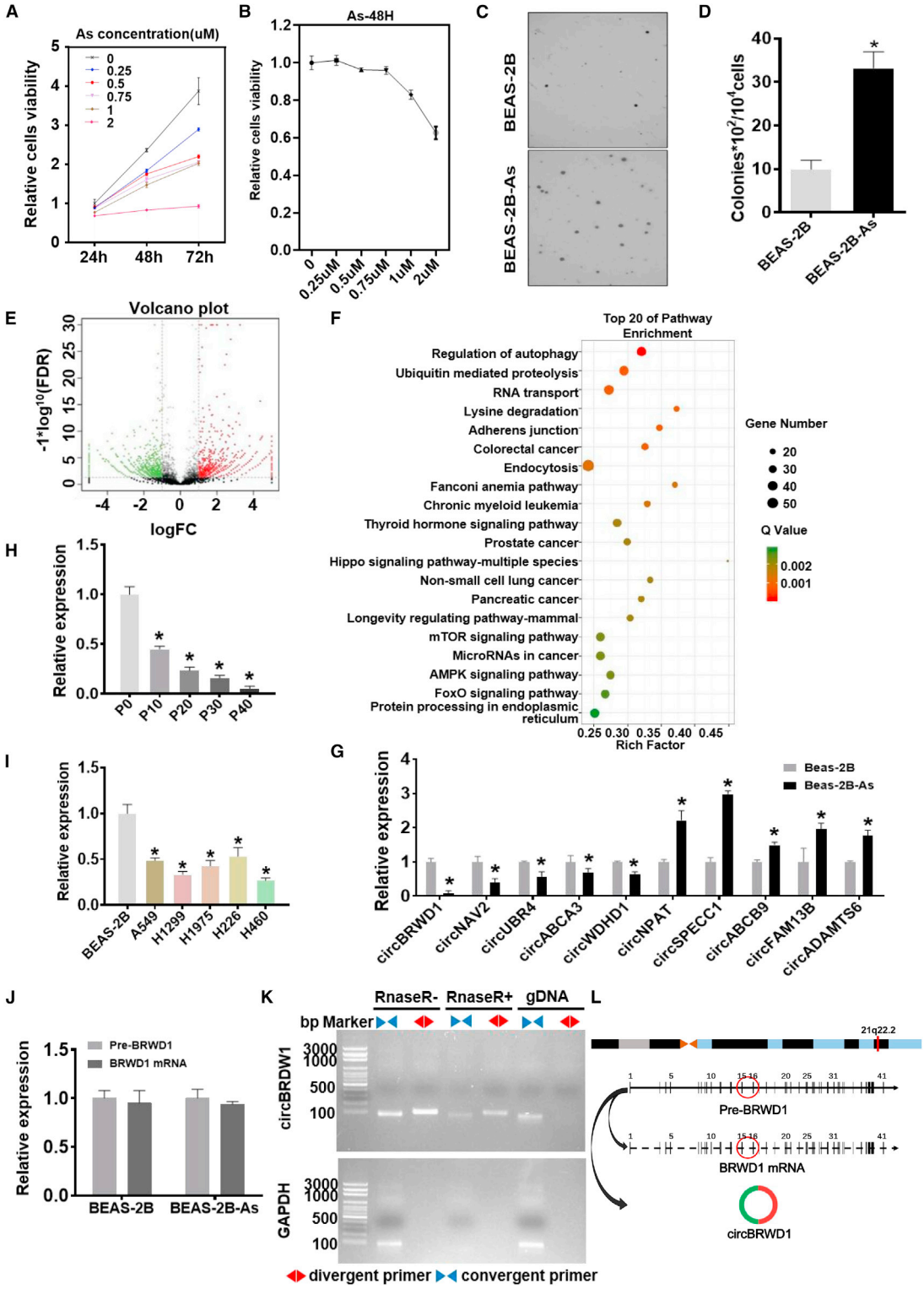

Figure 1. circBRWD1 is significantly downregulated in the malignant transformed cell model and lung cancer cell lines

(A and B) The viability of BEAS-2B cells treated with different concentrations of arsenic poison; the exposure times were tested by CCK-8 assay. (C and D) The ability of BEAS-2B cells exposed to arsenic and control BEAS-2B cells to grow on soft agar was observed under a microscope. (E) Volcano map showing the differential expression levels of

(legend continued on next page)

(EMT) modulation via endogenous competition mechanisms.[16] Recent studies have shown that chronic arsenic exposure might contribute to the malignant transformation of normal cells by regulating circRNA formation. For instance, the level of circRNA_100284 was increased and participated in the process of carcinogenesis in an arsenic-accelerated cell-cycle experiment.[13] Additionally, arsenic increases circLRP6 levels, binding to miR-455 and increasing ZEB1 expression, thus promoting EMT during malignant transformation.[17] Nevertheless, the mechanism through which arsenic regulates circRNAs and contributes to tumorigenesis remains enigmatic.

Three main molecular mechanisms of circRNA function have been revealed through recent research. First, circRNA acts as an miRNA sponge and regulates mRNA expression through miRNA sponging adsorption.[18] Second, circRNAs combine with proteins that form complexes that participate in cell proliferation, differentiation, and physiological activities such as apoptosis and oxidative stress.[19,20] Third, circRNAs directly encode small-molecule peptides that participate in the regulation of biological functions by influencing signaling pathways.[21,22] The clearest explanation for this action is circRNA acting as a sponge of miRNA, indirectly regulating mRNA expression; this regulatory mechanism has been confirmed with studies on arsenic carcinogenesis. circRNAs binding miRNAs mainly depends on nucleic acid sequence complementary pairing, but whether circRNAs can directly bind to mRNAs through the same base complementary pairing is currently unknown. Therefore, this study explores whether circRNAs can perform their function by directly binding and targeting mRNAs to regulate their expression. The function of circBRWD1 has not yet been revealed. The present study revealed that circBRWD1 is expressed at low levels in arsenic-induced human bronchial epithelial cells and multiple lung cancer cells that can inhibit the proliferation of malignantly transformed cells. The downregulation of circBRWD1 may be related to the development of lung cancer. In addition, the findings of this study explain the role of circRNA in the occurrence of lung cancer induced by arsenic exposure from the perspective of etiology. Our results provide new insights into the molecular mechanism of circRNAs in arsenic carcinogenesis.

RESULTS

circBRWD1 was significantly downregulated in a malignant transformation cell model and lung cancer cell lines

To investigate the potential mechanism of lung cancer caused by arsenic exposure, BEAS-2B cells were exposed to low-level arsenic poisoning to construct a malignantly transformed cell model (BEAS-2B-As) of lung cancer caused by arsenic exposure. To determine the optimal time of arsenic exposure, BEAS-2B cells were exposed to 0, 0.25, 0.5, 0.75, 1, and 2 μM $NaAsO_2$ and cultured for 24, 48, and 72 h. Then, a CCK-8 assay was performed to determine cell viability. The optimal arsenic exposure time of the BEAS-2B cells was determined to be 48 h (Figure 1A). To determine the no-observed-adverse-effect level (NOAEL) of arsenic exposure, BEAS-2B cells were exposed to 0, 0.25, 0.5, 0.75, 1, and 2 μM $NaAsO_2$ and cultured for 48 h. Then, a CCK-8 assay was performed to determine cell viability. The NOAEL was determined to be 0.75 μM $NaAsO_2$ (Figure 1B). Then, BEAS-2B cells were exposed to 0.75 μM $NaAsO_2$ continuously and cultured for 40 generations. Next, through soft agar colony formation experiments, it was found that the malignant proliferation of BEAS-2B-As cells after arsenic-induced malignant transformation was 3-fold that of normal cells (Figures 1C and 1D). The experimental results indicated that the model of the malignant transformation of bronchial epithelial cells induced by arsenic was successfully constructed.

With the in-depth study into the carcinogenic mechanism of arsenic and the continuous exploration of the biological functions of circRNAs, a great deal of evidence has shown that circRNA played a crucial role in the carcinogenesis induced by environmental pollutants, but the function and mechanism of circRNAs in the development of lung cancer caused by arsenic exposure have never been reported. Therefore, in this study, BEAS-2B-As cells were used as the experimental group, and BEAS-2B cells were used as the control group to perform RNA sequencing (Figures S1A and S1B) to analyze the differential expression of circRNAs. Compared with the control group consisting of BEAS-2B cells, there were 2,248 upregulated circRNAs and 2,354 downregulated circRNAs in BEAS-2B-As cells (Figures 1E and S1C). Subsequently, pathway enrichment analysis was performed on the differentially expressed genes. The analysis results indicated that the differentially expressed circRNAs were closely related to multiple signaling pathways that regulate tumor occurrence and development (Figures 1F and S1D). Considering the circRNA sequencing results, we selected 10 circRNAs with the most significantly different expression, of which 5 circRNAs were upregulated and 5 circRNAs were downregulated. qPCR was performed to determine the expression levels of these circRNAs in both BEAS-2B and BEAS-2B-As cells, and the results showed that circBRWD1 was the most significantly downregulated circRNA in BEAS-2B-As cells (Figure 1G). In addition, the expression of circBRWD1 in 0- (P0), 10- (P10), 20- (P20), 30- (P30), and 40-generation (P40) BEAS-2B cells exposed to arsenic was determined by qPCR, and it was clear that lung cancer was induced by arsenic exposure, with an increase in arsenic exposure per cell generation and a simultaneous trend of downward circBRWD1 expression becoming increasingly obvious

circRNAs. (F) The Kyoto Encyclopedia of Genes and Genomes (KEGG) website was used to conduct a pathway enrichment analysis of differentially expressed circRNAs. (G) The 10 most differentially expressed circRNAs in the expression profiles were verified by qPCR according to their expression levels in BEAS-2B cells and BEAS-2B-As cells. (H) circBRWD1 expression levels in BEAS-2B cells exposed to arsenic were detected by qPCR on the basis of cell generation P0, P10, P20, P30, and P40. (I) Compared with that in BEAS-2B cells, the expression of circBRWD1 in lung cancer cell lines (A549, H1299, H1975, H226, and H460 cell lines) was separately detected by qPCR. (J) The expression of pre-BRWD1 and BRWD1 mRNA in BEAS-2B cells and BEAS-2B-As cells was verified by qPCR. (K) After convergent and divergent primers were designed for PCR-agarose gel electrophoresis, the circular structure of circBRWD1 was confirmed. (L) Schematic structure of circBRWD1. An asterisk (*) indicates a significant difference ($p < 0.05$).

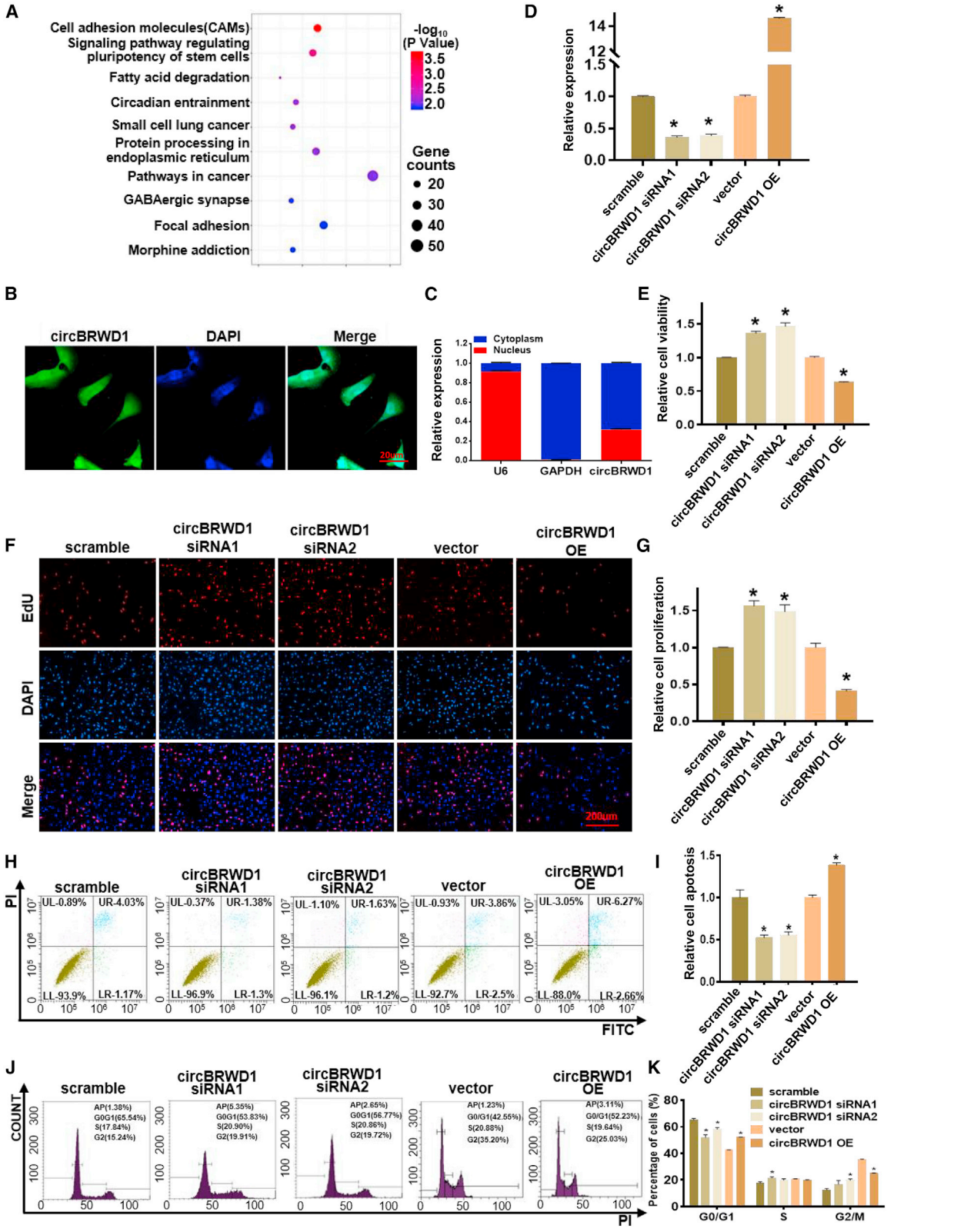

(legend on next page)

(Figure 1H). Then, we determined the expression of circBRWD1 in lung cancer cell lines, namely, the A549, H1299, H1975, H226, and H460 cell lines, and found that circBRWD1 was expressed at low levels in these lung cancer cell lines (Figure 1I). To distinguish circBRWD1 from linear pre-BRWD1 and BRWD1 mRNA, qPCR was performed, and the results showed that pre-BRWD1 and BRWD1 mRNA expression was not significantly different in BEAS-2B and BEAS-2B-As cells (Figure 1J), indicating that circBRWD1, as a closed circRNA, exhibited different biological functions than linear pre-BRWD1 and BRWD1 mRNA. To identify the circular structure of circBRWD1, we designed polymerized and dispersed primers, conducted agarose gel electrophoresis, and found that the divergent primers of circBRWD1 amplified only cDNA, not gDNA, while the divergent primers of GAPDH did not amplify either cDNA or gDNA (Figure 1K). The results verified the circular structure of circBRWD1. Analysis of the gene structure showed that the circBRWD1 circle-forming, back-splicing site, an annotated exon in circRNA, was located at the beginning of exon 15 and the terminating position of exon 16 of the pre-BRWD1 gene, and they were formed by back-splicing exons. (Figure 1L).

circBRWD1 significantly inhibited the proliferation of malignantly transformed cells

To explore the biological functions of circBRWD1 in lung cancer caused by arsenic, we performed pathway enrichment analysis on the basis of circBRWD1 expression (Figure 2A) and found that circBRWD1 participates in a variety of signaling pathways, especially cancer-related pathways, potentially participating in the process of lung cancer. Simultaneously, fluorescence *in situ* hybridization (FISH as well as nuclear and cytoplasmic fractionation examination revealed that circBRWD1 was distributed in both the cytoplasm and nucleus but was mainly localized in the cytoplasm (Figures 2B and 2C). To identify the *in vitro* function of circBRWD1, we transiently silenced and overexpressed it in BEAS-2B-As cells with circBRWD1-specific small interfering RNA (siRNA) and overexpression (OE) plasmids, respectively (Figure 2D). After silencing and OE efficiency verification, a CCK-8 assay was performed to determine the viability of BEAS-2B-As cells. In addition, an EdU assay was performed to determine the cell proliferation rate, and the cell apoptosis rate and cell-cycle progression were determined based on flow cytometry. Compared with the effect in the scramble group, silencing circBRWD1 promoted cell viability and proliferation, inhibited cell apoptosis, and accelerated the G0/G1 phase transition in BEAS-2B-As cells; however, its function was abrogated upon circBRWD1 OE (Figures 2E–2K). Furthermore, using a lentiviral vector, we constructed a BEAS-2B-As cell line that stably silenced or stably overexpressed circBRWD1 (Figure S2). The *in vitro* biological function of BEAS-2B-As cells, in which circBRWD1 was stably silenced or overexpressed, aligned with the effects of the transient silencing and OE of circBRWD1 (Figures 3A–3I). These experimental results showed that circBRWD1 participates in the regulation of the proliferation, cycle, and other functions of malignantly transformed lung cells, but the specific mechanisms of action in these processes need to be further explored.

circBRWD1 directly bound mRNA (c-JUN, c-MYC, and CDK6 mRNA) and affected its stability

According to recent molecular mechanism research, the best understood regulatory mechanism of circRNA involves its miRNA sponging action, through which circRNA indirectly changes the expression of mRNA by binding to miRNA. However, whether circRNAs directly bind to and regulate mRNAs remains unknown. By performing an RNA sequencing analysis (Figures S3A and S3B), we found a difference in the expression of genes between BEAS-2B and BEAS-2B-As cells and used these findings for further analysis. Compared with their counterparts in BEAS-2B cells, there were 3,508 upregulated mRNAs and 207 downregulated mRNAs in the model cells (Figures 4A, S3C, and S3D). The differentially expressed genes were assessed for pathway enrichment through pathway analysis. The analysis results showed that differentially expressed mRNAs were closely related to multiple pathways that are involved in tumor initiation and progression (Figures 4B and S3E). Through RIsearch1.1 analysis software coupled with the Linux operating system and IntaRNA and RNAcofold analysis tools used with the Windows operating system, the bioinformatics analysis results showed that circBRWD1 has the potential to bind directly to 23 mRNAs, including c-JUN, c-MYC, CDK6, and ACBD5 mRNA. According to the sequencing data, among these mRNAs, eight mRNAs exhibited differential expression (Figure 4C). Next, we validated the relationship between circBRWD1 and the eight mRNAs by performing qPCR experiments. After silencing circBRWD1, the mRNA expression levels of c-JUN, c-MYC, and CDK6 were significantly increased when compared with those in the scramble group. When circBRWD1 was transiently overexpressed, a significant decline in c-JUN, c-MYC, and CDK6 mRNA expression was evident. Our results showed that circBRWD1 negatively regulated the expression of c-JUN, c-MYC, and CDK6 (Figure 4D). Moreover, circBRWD1 showed the potential to directly bind and regulate mRNA. However, the nature of the binding relationship remains to be further explored.

We predicted a binding relationship between circBRWD1 and mRNA (c-JUN, c-MYC, CDK6 mRNA) based on website information

Figure 2. Transient silencing and overexpression of circBRWD1 significantly inhibited the proliferation of malignant transformed cells

(A) The KEGG website was used to conduct pathway enrichment analysis on circBRWD1. (B) FISH confirmed the subcellular localization of circBRWD1 in the cell; the nucleus was stained with DAPI, and circBRWD1 was labeled with a specific probe labeled with GFP. (C) The ratio of circBRWD1 expression in the nucleus and cytoplasm of BEAS-2B cells was determined; U6 served as a nuclear marker, while GAPDH was a cytoplasmic marker. (D) The efficiency of silencing or overexpressing circBRWD1 was measured after transient transfection with circBRWD1 siRNAs or the circBRWD1 overexpression vector into BEAS-2B-As cells. (E) After splicing and overexpressing circBRWD1, the viability of BEAS-2B-As cells was measured by CCK-8 assay. (F and G) EdU experiments measured the proliferation of BEAS-2B-As; cell nuclei were stained with DAPI. EdU/DAPI indicated the cell proliferation ability. (H–K) Flow cytometry was used to detect the apoptosis and cell cycle of BEAS-2B-As. An asterisk (*) indicates a significant difference ($p < 0.05$).

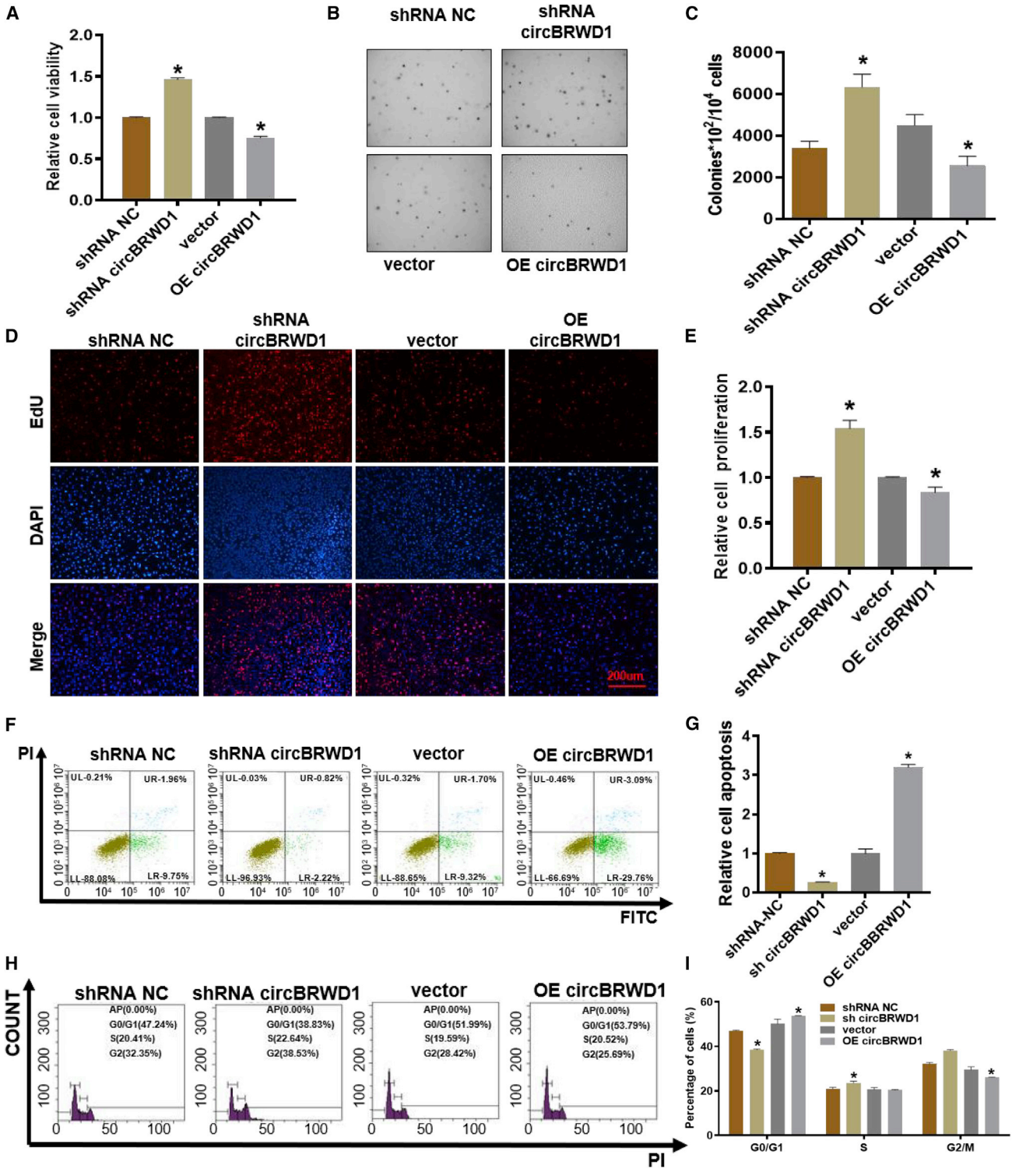

(legend on next page)

(http://rna.informatik.uni-freiburg.de/IntaRNA/Input.jsp). The specific binding area is shown in Figure 4E. According to the specific binding area of circBRWD1 and mRNA, we constructed a related luciferase reporter (Figure 4F) to verify the relationship between circBRWD1 and mRNA (c-JUN, c-MYC, and CDK6 mRNA). The intensity of the three-mRNA wild-type dual-luciferase reporter was significantly lower than that of the mutant reporter, which confirmed that circBRWD1 directly binds to c-JUN, c-MYC, and CDK6 (Figures 4G–4I). Then, an RNA antisense purification (RAP) experiment was used to further confirm the mRNAs that bound to circBRWD1. A schematic diagram of the RAP experiment is shown in Figure 4J. The results showed that the circBRWD1-specific probe significantly enriched circBRWD1 and enriched c-JUN, c-MYC, and CDK6 (Figure 4K). However, how does circBRWD1 affect the expression of c-JUN, c-MYC, and CDK6? We first explored whether circBRWD1 affects the mRNA stability of c-JUN, c-MYC, and CDK6 by using an mRNA stability test. The results showed that the stability of c-JUN, c-MYC, and CDK6 mRNA decreased after circBRWD1 was stably overexpressed (Figures 4L–4N). This decrease affected the expression of c-JUN, c-MYC, and CDK6 proteins (Figure 4O). These experimental results showed that circBRWD1 affects the stability of c-JUN, c-MYC, and CDK6 mRNA and regulates their expression levels by directly binding to them.

circBRWD1 regulated the proliferation of BEAS-2B-As cells by altering the expression of c-JUN, c-MYC, and CDK6

The aforementioned results indicate that circBRWD1 interacts directly with mRNAs (c-JUN, c-MYC, and CDK6) and regulates the protein expression of c-JUN, c-MYC, and CDK6 by affecting the stability of the corresponding mRNA. However, the underlying principle leading to this outcome, particularly the mechanism affecting the cell cycle and proliferation of BEAS-2B-As cells, remains largely unknown. We upregulated c-JUN, c-MYC, and CDK6 expression in BEAS-2B-As cells stably transfected with a circBRWD1 OE vector (Figure 5A). EdU assays showed that c-JUN, c-MYC, and CDK6 OE partially released the cells from the growth inhibition caused by the stable OE of circBRWD1 (Figures 5B and 5C). In addition, OE of c-JUN, c-MYC, and CDK6 decreased the proportion of cells in the G0/G1 phase that had been increased by circBRWD1 OE (Figures 5D and 5E). In BEAS-2B-As cells with stable circBRWD1 OE, c-JUN, and c-MYC, CDK6 OE restored the cell proliferation rate by regulating cell-cycle progression. Low expression of circBRWD1 mediated cell-cycle progression and accelerated the proliferation of lung carcinoma cells by affecting the mRNA stability and expression of c-JUN, c-MYC, and CDK6.

DISCUSSION

An increasing number of studies have shown that long-term exposure to low-dose arsenic can lead to the malignant transformation of multiple cell lines, such as human bronchial epithelial cells,[23] human embryonic lung fibroblasts,[24] and human keratinocytes.[25] The process of malignant cell transformation is closely related to the occurrence and development of tumors; therefore, a malignant transformation cell model is the best model for studying the mechanism of carcinogen-induced tumorigenesis. Malignant transformed cell models constructed by long-term low-dose arsenic exposure have been widely used to study the relevant mechanisms of arsenic-induced tumorigenesis.[26,27] To explore the mechanism of arsenic exposure-induced lung cancer, we constructed a malignant transformation model with human bronchial epithelial cells exposed to arsenic and performed a soft agar colony formation assay to verify the successful construction of the cell model.

Lung cancer is the leading cause of cancer-associated death worldwide.[1] However, the mechanisms underlying lung cancer progression have not yet been fully elucidated. Recent progress in RNA research has suggested that noncoding RNAs are involved in the progression of lung cancer.[28,29] The expression and abundance of circRNAs are tissue- and cell specific, which makes them more stable and specific than other noncoding RNAs.[30–32] A growing number of deregulated circRNAs have been identified and found to be involved in the development of tumors. Moreover, an increasing amount of evidence has shown that circRNAs play important roles in the carcinogenesis induced by environmental pollutants.[33,34] It has been reported that chronic arsenic exposure may participate in the malignant transformation of normal cells by regulating circRNA. For example, circRNA_100284 is involved in the malignant transformation of human keratinocytes and hepatocytes,[13,35] and both circLRP6 and circ00891 are involved in the malignant transformation of human keratinocytes. We provided the first evidence suggesting a molecular mechanism whereby circBRWD1 may affect the development of arsenic-induced lung cancer. In addition, during the malignant transformation of BEAS-2B cells induced by arsenic exposure, with an increase in arsenic exposure, the trend of circBRWD1 expression downregulation became increasingly obvious, and circBRWD1 was downregulated in five different lung cancer cell lines. By performing a bioinformatic analysis, we found that circBRWD1 may exert effects mediated by cancer-related pathways. Therefore, the biological functions of circBRWD1 were further investigated, and it was found that circBRWD1 regulated cell processes by regulating cell viability, apoptosis, and cell-cycle progression. These results indicate that circBRWD1 may be involved in the arsenic-induced malignant transformation of BEAS-2B cells.

Arsenic carcinogenesis is the result of an abnormal accumulation of many factors. It involves multiple genes, stages, and steps with changes in the structure and regulatory expression of a large number

Figure 3. circBRWD1 significantly inhibits the proliferation of malignant transformed cells (stable silencing and overexpression of circBRWD1 in BEAS-2B-As cells)

(A) A CCK-8 assay was performed to determine cell viability. (B and C) The change in cell growth ability on soft agar was assessed through observation with a microscope. (D and E) An EdU assay was performed to determine cell proliferation ability; DAPI stains the cell nucleus; EdU/DAPI staining indicates cell proliferation ability. (F–I) Flow cytometry was used to determine the cell cycle and apoptosis of cells. An asterisk (*) indicates a significant difference ($p < 0.05$).

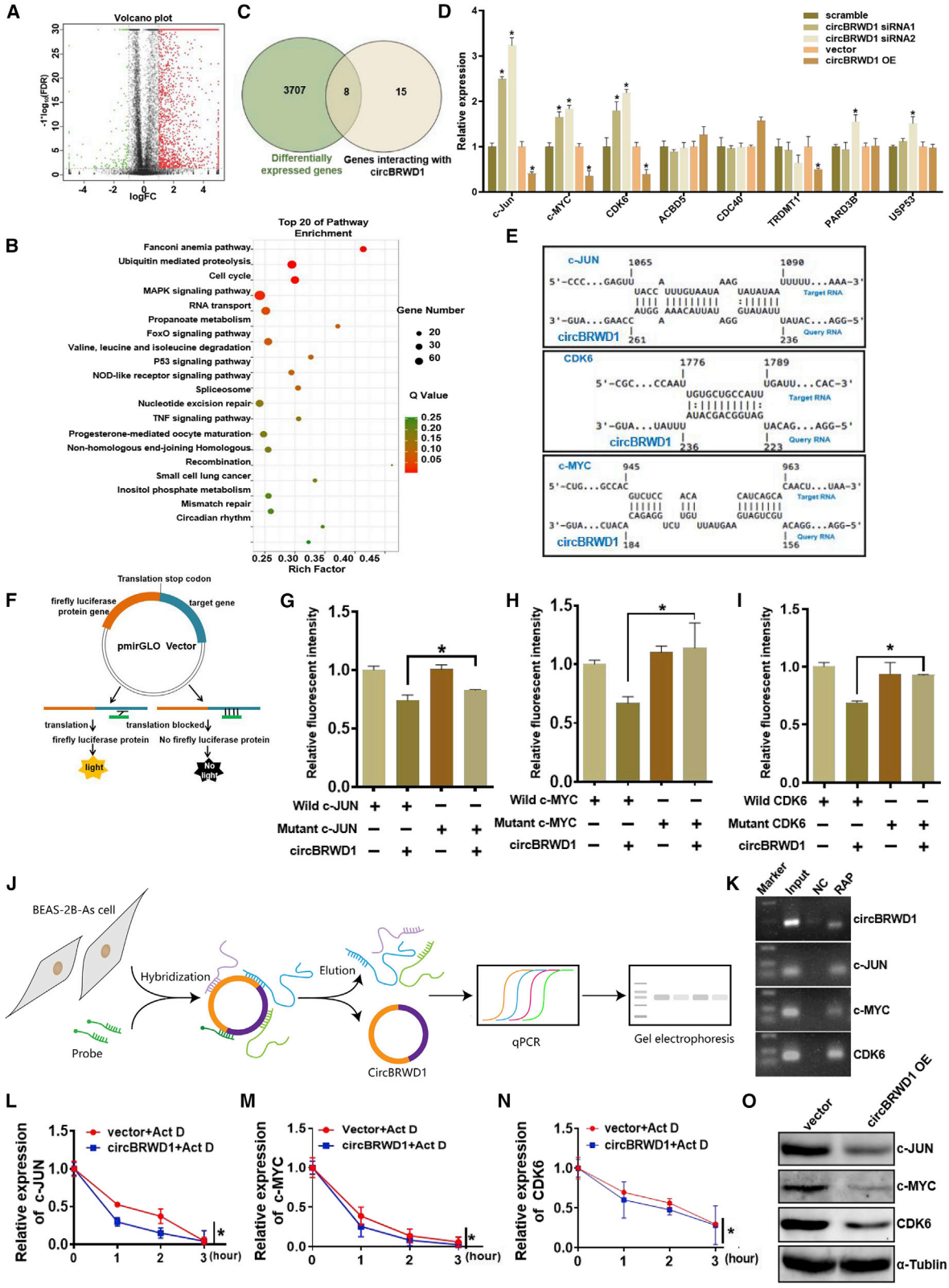

(legend on next page)

of related genes. Previous studies have shown that arsenic can participate in DNA-damage repair by regulating nucleotide excision repair (NER) and mismatch repair genes.[36] Oxidative damage caused by arsenic exposure can inhibit the expression of DNA polymerase β[37] and can cause DNA double-strand breaks.[38] Arsenic exposure-induced malignant transformation of HBE cells upregulated NRF2/NQO1 expression, increased cyclin E-CDK2 expression, accelerated the cell cycle, promoted cell proliferation, activated the NRF2/BCL-2 signaling pathway, and inhibited CHOP expression.[39] Arsenic exposure may influence the ROS/miR-199a-5p/HIF-1α/COX-2,[40] phosphoinositide 3′-kinase (PI3K)/Akt,[41] ROS/ERK/ELK1/MLCK, and ROS/p38 MAPK[42] pathways along with other pathways that induce carcinogenesis. Chronic arsenic exposure may contribute to malignant transformation through miRNA-mediated autophagy, angiogenesis, and apoptosis pathway activation.[11] Recent studies have shown that arsenic can cause cancer by regulating the abnormal expression of circRNA. Xue et al. found that arsenic exposure increased the expression of circ100284, which sponged miR-217, upregulating the expression of the miR-217 target EZH2, which in turn upregulated cyclin D1 and CDK4 expression, thereby accelerating the cell cycle and leading to malignant cell transformation.[35] In another study, long-term exposure to low-concentration arsenic increased the expression of circRNA_100284, which accelerated cell proliferation and shortened the cell cycle, ultimately leading to the malignant transformation of L-02 cells.[13] circ008913 was downregulated in arsenic-exposed malignantly transformed immortalized human keratinocytes, sponged miR-889, and regulated DAB2IP/ZEB1, contributing to the carcinogenic process induced by arsenic.[33] However, the mechanism by which circRNA contributes to arsenic-induced lung cancer has not yet been reported.

A vast amount of research has shown that circRNAs can regulate the occurrence and development of lung cancer.[43,44] Among the molecular mechanisms by which circRNA functions have been clearly revealed through recent research, circRNA sponging of miRNA, which indirectly regulates mRNA expression by adsorbing the miRNA, predominates, with this regulatory mechanism confirmed to affect arsenic-induced carcinogenesis.[13,35] However, whether circRNAs perform their functions by directly binding and targeting mRNAs and regulating their expression remains largely unknown. In this study, we performed RNA sequencing with malignantly transformed BEAS-2B-As cells and control BEAS-2B cells to analyze changes in their expression profiles. Pathway enrichment analysis revealed that differential mRNAs are closely related to multiple signaling pathways that regulate tumor occurrence and development. In this study, we found that circBRWD1 can negatively regulate the expression of mRNA (c-JUN, c-MYC, and CDK6 mRNA), and further study showed that circBRWD1 can interact with mRNA (c-JUN, c-MYC, and CDK6 mRNA), affecting its stability and thus regulating the protein levels of c-JUN, c-MYC, and CDK6.

c-JUN is encoded by the c-JUN proto-oncogene and plays a central role in cell signal transduction. It positively regulates cell proliferation by inhibiting the expression of tumor suppressor genes.[45,46] Activation of the JNK/c-JUN signaling pathway is associated with cancer progression.[47,48] The circ_100984-miR-432-3p axis regulates the c-Jun/YBX-1/β-catenin feedback loop to promote the progression of bladder cancer and provides a potential therapeutic axis for bladder cancer.[49] c-MYC is one of the most frequently activated oncogenes, and the dysregulation of this oncogene is associated with a variety of human cancers.[50,51] Furthermore, circRNAs activate the energy metabolism of osteosarcoma by regulating the c-MYC signaling pathway,[52] promote the development of breast cancer,[20,53] and inhibit the growth and migration of bladder cancer cells.[54] CDK6 is a classic protein involved in cell-cycle regulation, specifically promoting cell proliferation by accelerating the cell cycle. Upregulation of hsa_circ_0136666 promotes breast cancer development because it is an miR-1299 sponge and targets CDK6.[55] Chi-Wen Luo et al. found that the CDK6-c-Jun-Sp1-MMP-2 axis can be used as a biomarker and therapeutic target for triple-negative breast cancer.[56] Increasing evidence shows that circRNAs regulate the occurrence and development of cancer through signaling pathways involving c-JUN, c-MYC, and CDK6. Our research revealed that circBRWD1 directly binds to mRNA (c-JUN, c-MYC, and CDK6 mRNA) and affects its stability. Subsequently, circBRWD1 combined with c-JUN, c-MYC, and CDK6 was stably overexpressed in the arsenic-induced malignant transformation model of BEAS-2B cells. The cell cycle was restored, reestablishing the proliferation ability of these cells and confirming that a low level of circBRWD1 expression affects the cell cycle by modulating the stability of c-JUN, c-MYC, and CDK6 mRNA, thereby accelerating the proliferation of lung cancer cells.

Lung cancer is the main cause of cancer-related death worldwide and has thus been a focus of cancer research. Exposure to environmental chemical carcinogens is an important factor in tumorigenesis. Understanding carcinogenic molecular mechanisms is of great importance to find an increasing number of effective early diagnostic markers and therapeutic targets. To date, few studies have reported the function

Figure 4. circBRWD1 directly binds to mRNA (c-JUN, c-MYC, and CDK6 mRNA) and affects its stability

(A) Volcano plot showing differentially expressed mRNAs. (B) Pathway enrichment analysis of differentially expressed mRNAs with the KEGG website. (C) Bioinformatics analysis of mRNAs that can directly bind to circBRWD1. (D) The relationship between circBRWD1 and the expression of eight mRNAs was assessed by qPCR. (E) Specific assembly area. (F) Schematic diagram of the experimental vector carrying the dual luciferase reporter gene. (G–I) The binding sites in circBRWD1 for c-JUN, c-MYC, and CDK6 were mutated, and the dual-luciferase reporter gene was used for detection. (J) Schematic diagram of the RAP experiment. (K) After the RAP experiment, circBRWD1, c-JUN, c-MYC, and CDK6 expression was measured by qPCR, and the qPCR products were subjected to nucleic acid gel electrophoresis using a 1% agarose gel. (L–N) Actinomycin D (ActD) was added to BEAS-2B-As and control cells stably overexpressing circBRWD1. Cell RNA was extracted at different time points (0, 1, 2, and 3 h), and mRNA (c-JUN, c-MYC, and CDK6 mRNA) was detected by qPCR. (O) Western blot analysis was performed to determine the protein expression of c-JUN, c-MYC, and CDK6 after transient overexpression of circBRWD1. An asterisk (*) indicates a significant difference ($p < 0.05$).

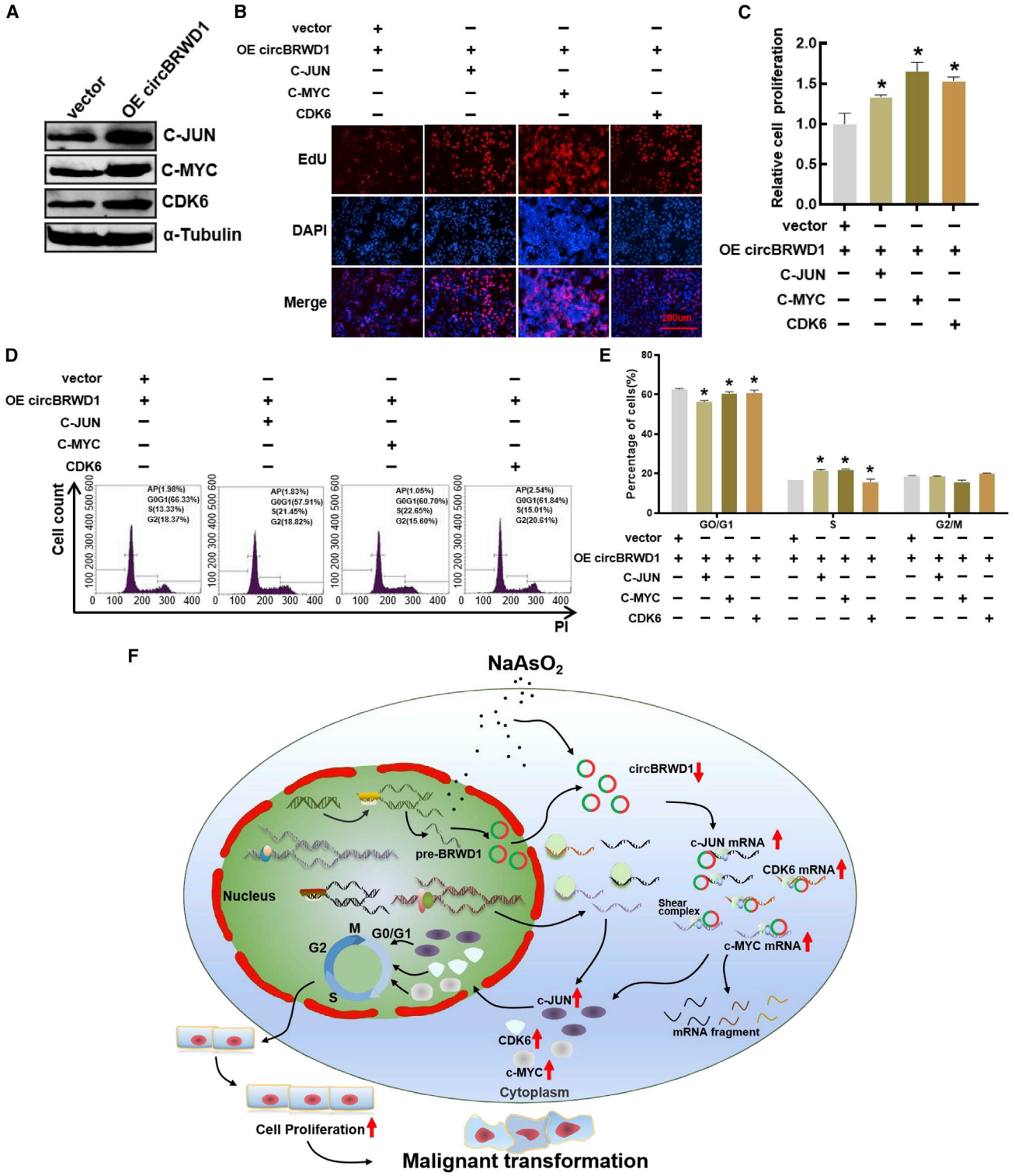

Figure 5. circBRWD1 regulates the proliferation of malignantly transformed cells by downregulating c-JUN, c-MYC, and CDK6

(A) Western blot analysis of the expression of c-JUN, c-MYC, and CDK6 in the BEAS-2B-As cell line stably overexpressing circBRWD1. (B and C) An EdU assay was performed to determine the cell proliferation ability of BEAS-2B-As cells stably overexpressing circBRWD1 and c-JUN, c-MYC, and CDK6; DAPI stains the nucleus;

(legend continued on next page)

of circRNAs in the development of lung cancer caused by arsenic exposure. This study explained the function of circRNAs in the development of lung cancer caused by arsenic exposure from an etiological point of view. circBRWD1 is downregulated under arsenic exposure, which leads to increased stability of its targeted mRNA (c-JUN, c-MYC, or CDK6 mRNA), upregulating its expression, promoting the malignant transformation of human bronchial epithelial cells, and eventually leading to the occurrence of lung cancer (Figure 5F). circBRWD1 can directly bind and target the regulatory factors critical to mRNA stability, thereby regulating the expression of multiple genes, a principle that is essential for clarifying the molecular mechanism of arsenic-induced lung cancer. Clarifying the molecular mechanism of key regulatory factors involved in arsenic-induced lung cancer provides new insights into the prevention and treatment of lung cancer.

MATERIALS AND METHODS

Cell culture and establishment of an arsenic-exposed malignant transformation cell model

Human bronchial epithelial cells (BEAS-2B), lung cancer cell lines (A549, H460, H1299, H226, and H1975 cell lines), and embryonic kidney cells (293T cells) were purchased from American Type Culture Collection (ATCC, Manassas, VA, USA), Guangzhou Saiku Biotechnology (Guangzhou, China), and Cell Bank of Shanghai Academy of Chinese Sciences, respectively. BEME (Clonetics, CC-3171) was used with a BEGM kit to establish the BEAS-2B cell culture. RPMI-1640 medium (Gibco, C11875500BT) containing 10% fetal bovine serum (Gibco, 10099141C) and 1% streptomycin/penicillin (Gibco, 15140122) was used for culturing H460, H1975, H226, and H1299 cells, and Ham's F12 medium (Gibco, 21127022) containing 10% fetal bovine serum and 1% streptomycin/penicillin was used for culturing A549 cells. All cell lines were incubated at 37°C in a humidified incubator containing 5% CO_2. For chronic arsenic exposure, BEAS-2B cells were continuously exposed to arsenic (0.75 μM $NaAsO_2$). After reaching approximately 80%–90% confluence after 48 h of arsenic exposure, the cells were subcultured. The degree of cell transformation ability and the level of tumorigenicity were confirmed by a soft agar formation assay.

RNA sequencing

Total RNA was isolated from BEAS-2B and BEAS-2B-As cells and used for sequencing library construction. To summarize, the RNAs were fragmented into short sections in the fragmentation buffer and then converted into 1st-strand cDNA via reverse transcription with random hexamer primers. Second-strand cDNA was synthesized by deoxynucleoside triphosphate (dNTP), RNase H, DNA polymerase I, and the buffer. QiaQuick PCR was used to purify the cDNA fragments, the ends were repaired, and base A was introduced and ligated into Illumina sequencing adapters. The ligation products were selected through agarose gel electrophoresis based on size, amplified by PCR, and sequenced using the Illumina HiSeqTM 2500 Gene Denovo Biotechnology (Guangzhou, China).

Total RNA extraction, reverse transcription, and qPCR

Total RNA was isolated using TRIzol Reagent (Invitrogen, 15596018) according to manufacturer protocols. The quality and concentration of the purified total RNAs were detected using a Nanodrop One detection system (Thermo Fisher Scientific) and then reverse transcribed using a GoScript Reverse Transcription System (Promega, A5002). qPCR was carried out using GoTaq qPCR Master Mix (Promega, A6001) according to manufacturer instructions on an Applied Biosystems QuantStudio 7 Flex Real-Time PCR System (Thermo Fisher Scientific). GAPDH was used as the internal reference. The primers were synthesized by Sangon Biotech. The $2^{-\triangle\triangle Ct}$ method was used to calculate the relative expression. All primer sequences are shown in Table S1.

Plasmid construction

A plasmid used for overexpressing circBRWD1 and an empty control plasmid (pcDNA3.1) were purchased from Hunan Fenghui Biotechnology, China, and plasmid sequences were verified via sequencing. Transformed *Escherichia coli* was added to Luria-Bertani medium (LB) medium (5 g/L yeast powder [Solarbio, Y8020], 10 g/L sodium chloride [Aladdin, C111533], and 5 g/L tryptone [Solarbio, T8490]) and incubated on a shaker for 14 h. Plasmid extraction was performed using a Plasmid Midi Kit (QIAGEN, 12145) according to manufacturer instructions.

Transfection experiment

The OE plasmid and pcDNA3.1 (negative control) were transfected using Lipofectamine 3000 Transfection Reagent (Invitrogen, L3000015) according to manufacturer protocols. siRNAs targeting circBRWD1 and scramble controls were synthesized by GenePharma, China. siRNA was transfected into cells using a riboFECT CP Transfection Kit (RiboBio, C10511-05) according to manufacturer instructions. The transfection efficiency was determined by qPCR. All siRNA sequences are shown in Table S1.

Establishment of stably transfected circBRWD1-expressing cell lines

Stable lentivirus short hairpin (shRNA)-circBRWD1 and lentivirus OE-circBRWD1 vectors were constructed and packaged into lentiviruses. Lentiviral vectors, including shRNA-NC (the control for the knockdown group), shRNA-circBRWD1 (with circBRWD1 knockdown), empty (the control for the OE group), and OE-circBRWD1 (circBRWD1 overexpressing) vectors, were used to infect cells. Cells were incubated for more than 48 h, and fluorescence signals were observed using a fluorescence microscope (AMG EVOS, Mill Creek, WA, USA). Monoclonal was used to select stable strains.

EdU/DAPI indicates cell proliferation ability. (D and E) With the overexpression of c-JUN, c-MYC, and CDK6 in the BEAS-2B-As cell line stably overexpressing circBRWD1, PI staining and flow cytometry were used to identify cell-cycle changes. (F) The mechanism of action of circBRWD1 in the development of lung cancer induced by arsenic. An asterisk (*) indicates a significant difference ($p < 0.05$).

Cell viability test

The cell viability test was conducted with a Cell Counting Kit-8 (CCK8, Dojindo, CK04). Briefly, CCK-8 reagent was added and mixed with the culture medium at a ratio of 1:10. This mixture was added to the cells in the blank group, control group, and experimental group. After the cells were incubated in this CCK-8-containing medium for 2 h at 37°C, the absorbency was measured at 450 nm. For the viability test, cells were exposed to different concentrations of 0.25, 0.5, 0.75, 1, and 2 μM $NaAsO_2$ for 24, 48, and 72 h.

Verification of the circRNA structure

The circRNA structure was confirmed by a linear RNA digestion enzyme (RNase R) assay and convergent and divergent primer verification. In summary, the linear RNA digestion enzyme RNase R (Epicenter, RNR07250) was incubated at 37°C for 15 min at a dose of 3 U RNase R/μg RNA to degrade linear RNA and verify the resistance of circRNA to RNase R treatment. Finally, PCR (Aidlab, PC5001) and gel electrophoresis were performed with convergent and divergent primers to verify the circular structure of circBRWD1.

FISH

The subcellular localization of circBRWD1 was analyzed with a FISH kit (RiboBio, C10910). A specific circBRWD1 FISH probe labeled with a 5′-FAM-modified specific probe was synthesized by Sangon Biotech. The specific circBRWD1 FISH probe sequences are shown in Table S1. Cells were attached to slides, fixed with 4% paraformaldehyde, washed with PBS, and then permeabilized with a precooled permeabilizing agent (0.5% Triton X-100 in PBS) at 4°C for 5 min. The prehybridization solution was used to block cells for 30 min at 37°C, and then the hybridization solution containing 20 nM circBRWD1-specific FISH probe was incubated at 42°C overnight in the dark. DAPI staining solution was performed for 10 min at room temperature after the coverslips were washed. Images were obtained using an LSM800 confocal microscope (ZEISS) to analyze the subcellular localization of circBRWD1.

Nuclear and cytoplasmic separation

Nuclear and cytoplasmic separation was performed using a PARIS kit (Invitrogen, AM1921) according to manufacturer instructions. circBRWD1 expression was measured to further determine its subcellular localization. U6 served as a nuclear marker, while GAPDH served as a cytoplasmic marker.

EdU assay

An EdU assay was performed to measure cell proliferation with a Cell-Light EdU Apollo567 In Vitro Kit (RiboBio, C10310-1). Images were captured using an EVOS FL Auto Imaging System. Cell proliferation was determined by the proportion of EdU-positive cells in the DAPI-positive cell population. Finally, the relative cell proliferation calculation formula was used on the basis of the cell proliferation parameter that was measured in the control group. The calculations were then standardized and compared between the groups.

Flow cytometry analysis

Apoptosis was detected using an Annexin V-FITC/PI double-staining apoptosis detection kit (KeyGen Biotech, KGA107) according to manufacturer instructions. Cells were collected after treatment with trypsin without EDTA (Solarbio, T1350) and washed once with PBS. The cell pellet was resuspended in binding buffer, and 5 μL Annexin V-FITC and PI staining agents were added and incubated for 15 and 5 min in the dark, respectively. Then, the apoptosis rate of each group was determined with data obtained with a CytoFLEX Flow Cytometer (Beckman Coulter).

For cell-cycle analysis, cells were fixed in 70% ice-cold ethanol overnight. Next, 30 μL RNase A (Epicenter, RNR07250) was incubated with the cells at 37°C for 30 min. The cells were then stained at 4°C for 30 min with 120 μL PI (KeyGen Biotech, KGA512) in the dark. Fluorescence intensity was measured using a CytoFLEX Flow Cytometer (Beckman Coulter). The proportion of cells in the G0/G1, S, and G2/M cell-cycle phases was determined, and the proportions were then compared.

Dual-luciferase reporter assay

Wild-type and mutant luciferase reporter gene vectors of mRNA (c-JUN, c-MYC, and CDK6 mRNA) were constructed by Hunan Fenghui Biotechnology, China. HEK-293T cells were seeded in 12-well plates and cultured for 24 h, then circBRWD1 was cotransfected with wild-type vector and mutant vector into 293T cells. After 24 h of incubation, the luciferase activity of each treatment group was detected with a Dual-Luciferase Reporter Assay System (Promega, E1910). Fluorescein fluorescence was used to normalize Renilla fluorescence.

RAP

The RAP assay was performed using a RAP kit (BersinBio, Bes5103) according to manufacturer instructions. Three circBRWD1-specific RAP probes were designed and synthesized by Sangon Biotech. The specific probe sequences are shown in Table S1. Briefly, 4×10^7 cells were harvested, 40 mL 1% formaldehyde in PBS was used for crosslinking at room temperature for 10 min, and 0.4 g glycine was added to neutralize the crosslinking reaction for 5 min. Then, cell pellets were collected and lysed with lysis buffer, protease inhibitor, and RNase inhibitor. After removing DNA and hybridizing with probes, biotin-labeled magnetic beads were added to capture circBRWD1 and its conjugate. Then, candidate mRNA expression in the circBRWD1 conjugate was analyzed.

mRNA stability test

A specific number of experimental cells was plated in a 6-well plate. Actinomycin (ActD; 10 μg/mL) was added when the cell density was approximately 90%. Cell RNA was collected 0, 1, 2, and 3 h after treatment, and then 1 mL TRIzol reagent was added to lyse the cells. Cellular RNA was extracted and reverse transcribed, and the mRNA degradation rate was determined by qPCR.

Western blot analysis

Cell lysis buffer (10 mM Tris-HCl [pH 7.4], 1% SDS, and 1 mM Na_3VO_4) was used to lyse cells and extract protein. Total proteins

were evaluated with a Pierce BCA protein assay kit (Thermo Fisher Scientific, 23227). Dodecyl sulfate-polyacrylamide gels were used for electrophoresis to separate proteins. Then, each protein was electroblotted onto polyvinylidene fluoride (PVDF) membranes. Primary antibody was incubated overnight with the membranes at 4°C after skim milk was used to block the PVDF membrane. The PVDF membrane was then incubated with goat anti-mouse IgG (1:5,000, Proteintech, SA00001-1) or goat anti-rabbit IgG (1:5,000, Cell Signaling Technology, 7074S). Finally, chemiluminescence imaging was performed with a Clinx S6 system; the gray value analysis of the protein bands was performed with ImageJ software.

Statistical analysis

The data are presented as the means ± standard deviations (SDs) in our study. The statistical analysis was performed with SPSS (19.0), and the statistical graphs were generated with GraphPad Prism 7 software. Comparison of quantitative data between two groups was performed by t test or rank-sum test. All statistical analyses were two-sided tests, and a p value <0.05 was set as the statistically significant difference.

Data availability

All data used during the current study available from the corresponding author upon reasonable request.

SUPPLEMENTAL INFORMATION

Supplemental information can be found online at https://doi.org/10.1016/j.omto.2022.08.006.

ACKNOWLEDGMENTS

This work was partially supported by the National Natural Science Foundation of China (NSFC81903356) and Guangxi Science and Technology Base and Talent Special Project (no.AD22080055).

AUTHOR CONTRIBUTIONS

A.N. supervised paper creation and reviewed and revised the manuscript. X.L. and S.C. performed the main experiments, analyzed the data, and wrote, reviewed, and revised the manuscript. X.L. and X.W. conceived and designed the research. X.W. assisted with the experiments and assisted in analyzing the data. R.Z. reviewed and revised the manuscript. J.Y., H.X., W.H., M.L., and S.W. revised the manuscript.

DECLARATION OF INTERESTS

The authors declare that they have no known competing financial interests or personal relationships that may have influenced the work reported in this paper.

REFERENCES

1. Sung, H., Ferlay, J., Siegel, R.L., Laversanne, M., Soerjomataram, I., Jemal, A., and Bray, F. (2021). Global Cancer Statistics 2020: GLOBOCAN estimates of incidence and mortality worldwide for 36 cancers in 185 countries. CA. Cancer J. Clin. *71*, 209–249.
2. Naujokas, M.F., Anderson, B., Ahsan, H., Aposhian, H.V., Graziano, J.H., Thompson, C., and Suk, W.A. (2013). The broad scope of health effects from chronic arsenic exposure: update on a worldwide public health problem. Environ. Health Perspect. *121*, 295–302.
3. Maheshwari, N., Khan, F.H., and Mahmood, R. (2017). Sodium meta-arsenite induced reactive oxygen species in human red blood cells: impaired antioxidant and membrane redox systems, haemoglobin oxidation, and morphological changes. Free Radic. Res. *51*, 483–497.
4. Karachaliou, C., Sgourou, A., Kakkos, S., and Kalavrouziotis, I. (2021). Arsenic exposure promotes the emergence of cardiovascular diseases. Rev. Environ. Health. https://doi.org/10.1515/reveh-2021-0004.
5. Salmeri, N., Villanacci, R., Ottolina, J., Bartiromo, L., Cavoretto, P., Dolci, C., Lembo, R., Schimberni, M., Valsecchi, L., Viganò, P., and Candiani, M. (2020). Maternal arsenic exposure and gestational diabetes: a systematic review and meta-analysis. Nutrients *12*, E3094.
6. Wei, S., Zhang, H., and Tao, S. (2019). A review of arsenic exposure and lung cancer. Toxicol. Res. *8*, 319–327.
7. Lamm, S.H., Boroje, I.J., Ferdosi, H., and Ahn, J. (2021). A review of low-dose arsenic risks and human cancers. Toxicology *456*, 152768.
8. Kojima, C., Ramirez, D.C., Tokar, E.J., Himeno, S., Drobná, Z., Stýblo, M., Mason, R.P., and Waalkes, M.P. (2009). Requirement of arsenic biomethylation for oxidative DNA damage. J. Natl. Cancer Inst. *101*, 1670–1681.
9. Konkel, L. (2015). Inner workings of arsenic: DNA methylation targets offer clues to mechanisms of toxicity. Environ. Health Perspect. *123*, A21.
10. Medda, N., De, S.K., and Maiti, S. (2021). Different mechanisms of arsenic related signaling in cellular proliferation, apoptosis and neo-plastic transformation. Ecotoxicol. Environ. Saf. *208*, 111752.
11. Ferragut Cardoso, A.P., Udoh, K.T., and States, J.C. (2020). Arsenic-induced changes in miRNA expression in cancer and other diseases. Toxicol. Appl. Pharmacol. *409*, 115306.
12. Xiao, T., Zou, Z., Xue, J., Syed, B.M., Sun, J., Dai, X., Shi, M., Li, J., Wei, S., Tang, H., et al. (2021). LncRNA H19-mediated M2 polarization of macrophages promotes myofibroblast differentiation in pulmonary fibrosis induced by arsenic exposure. Environ. Pollut. *268*, 115810.
13. Dai, X., Chen, C., Yang, Q., Xue, J., Chen, X., Sun, B., Luo, F., Liu, X., Xiao, T., Xu, H., et al. (2018). Exosomal circRNA_100284 from arsenite-transformed cells, via microRNA-217 regulation of EZH2, is involved in the malignant transformation of human hepatic cells by accelerating the cell cycle and promoting cell proliferation. Cell Death Dis. *9*, 454.
14. Conn, V.M., Hugouvieux, V., Nayak, A., Conos, S.A., Capovilla, G., Cildir, G., Jourdain, A., Tergaonkar, V., Schmid, M., Zubieta, C., and Conn, S.J. (2017). A circRNA from SEPALLATA3 regulates splicing of its cognate mRNA through R-loop formation. Nat. Plants *3*, 17053.
15. Jeck, W.R., and Sharpless, N.E. (2014). Detecting and characterizing circular RNAs. Nat. Biotechnol. *32*, 453–461.
16. Wang, H., Feng, L., Cheng, D., Zheng, Y., Xie, Y., and Fu, B. (2021). Circular RNA MAT2B promotes migration, invasion and epithelial-mesenchymal transition of non-small cell lung cancer cells by sponging miR-431. Cell Cycle *20*, 1617–1627.
17. Xue, J., Chen, C., Luo, F., Pan, X., Xu, H., Yang, P., Sun, Q., Liu, X., Lu, L., Yang, Q., et al. (2018). CircLRP6 regulation of ZEB1 via miR-455 is involved in the epithelial-mesenchymal transition during arsenite-induced malignant transformation of human keratinocytes. Toxicol. Sci. *162*, 450–461.
18. Hansen, T.B., Jensen, T.I., Clausen, B.H., Bramsen, J.B., Finsen, B., Damgaard, C.K., and Kjems, J. (2013). Natural RNA circles function as efficient microRNA sponges. Nature *495*, 384–388.
19. Du, W.W., Yang, W., Liu, E., Yang, Z., Dhaliwal, P., and Yang, B.B. (2016). Foxo3 circular RNA retards cell cycle progression via forming ternary complexes with p21 and CDK2. Nucleic Acids Res. *44*, 2846–2858.
20. Wang, X., Chen, M., and Fang, L. (2021). hsa_circ_0068631 promotes breast cancer progression through c-Myc by binding to EIF4A3. Mol. Ther. Nucleic Acids *26*, 122–134.

21. Yang, Y., Gao, X., Zhang, M., Yan, S., Sun, C., Xiao, F., Huang, N., Yang, X., Zhao, K., Zhou, H., et al. (2018). Novel role of FBXW7 circular RNA in repressing glioma tumorigenesis. J. Natl. Cancer Inst. *110*, 304–315.

22. Zhang, M., Huang, N., Yang, X., Luo, J., Yan, S., Xiao, F., Chen, W., Gao, X., Zhao, K., Zhou, H., et al. (2018). A novel protein encoded by the circular form of the SHPRH gene suppresses glioma tumorigenesis. Oncogene *37*, 1805–1814.

23. Park, Y.H., Kim, D., Dai, J., and Zhang, Z. (2015). Human bronchial epithelial BEAS-2B cells, an appropriate in vitro model to study heavy metals induced carcinogenesis. Toxicol. Appl. Pharmacol. *287*, 240–245.

24. Li, Y., Shen, L., Xu, H., Pang, Y., Xu, Y., Ling, M., Zhou, J., Wang, X., and Liu, Q. (2011). Up-regulation of cyclin D1 by JNK1/c-Jun is involved in tumorigenesis of human embryo lung fibroblast cells induced by a low concentration of arsenite. Toxicol. Lett. *206*, 113–120.

25. Li, Y., Jiang, R., Zhao, Y., Xu, Y., Ling, M., Pang, Y., Shen, L., Zhou, Y., Zhang, J., Zhou, J., et al. (2012). Opposed arsenite-mediated regulation of p53-survivin is involved in neoplastic transformation, DNA damage, or apoptosis in human keratinocytes. Toxicology *300*, 121–131.

26. Chen, C., Jiang, X., Gu, S., and Zhang, Z. (2017). MicroRNA-155 regulates arsenite-induced malignant transformation by targeting Nrf2-mediated oxidative damage in human bronchial epithelial cells. Toxicol. Lett. *278*, 38–47.

27. Sun, M., Tan, J., Wang, M., Wen, W., and He, Y. (2021). Inorganic arsenic-mediated upregulation of AS3MT promotes proliferation of nonsmall cell lung cancer cells by regulating cell cycle genes. Environ. Toxicol. *36*, 204–212.

28. Qian, X., Yang, J., Qiu, Q., Li, X., Jiang, C., Li, J., Dong, L., Ying, K., Lu, B., Chen, E., et al. (2021). LCAT3, a novel m6A-regulated long non-coding RNA, plays an oncogenic role in lung cancer via binding with FUBP1 to activate c-MYC. J. Hematol. Oncol. *14*, 112.

29. Iqbal, M.A., Arora, S., Prakasam, G., Calin, G.A., and Syed, M.A. (2019). MicroRNA in lung cancer: role, mechanisms, pathways and therapeutic relevance. Mol. Aspects Med. *70*, 3–20.

30. Salzman, J., Chen, R.E., Olsen, M.N., Wang, P.L., and Brown, P.O. (2013). Cell-type specific features of circular RNA expression. PLoS Genet. *9*, e1003777.

31. Liu, J., Liu, T., Wang, X., and He, A. (2017). Circles reshaping the RNA world: from waste to treasure. Mol. Cancer *16*, 58.

32. Jeck, W.R., Sorrentino, J.A., Wang, K., Slevin, M.K., Burd, C.E., Liu, J., Marzluff, W.F., and Sharpless, N.E. (2013). Circular RNAs are abundant, conserved, and associated with ALU repeats. RNA *19*, 141–157.

33. Xiao, T., Xue, J., Shi, M., Chen, C., Luo, F., Xu, H., Chen, X., Sun, B., Sun, Q., Yang, Q., et al. (2018). Circ008913, via miR-889 regulation of DAB2IP/ZEB1, is involved in the arsenite-induced acquisition of CSC-like properties by human keratinocytes in carcinogenesis. Metallomics. *10*, 1328–1338.

34. Caiment, F., Gaj, S., Claessen, S., and Kleinjans, J. (2015). High-throughput data integration of RNA-miRNA-circRNA reveals novel insights into mechanisms of benzo[a]pyrene-induced carcinogenicity. Nucleic Acids Res. *43*, 2525–2534.

35. Xue, J., Liu, Y., Luo, F., Lu, X., Xu, H., Liu, X., Lu, L., Yang, Q., Chen, C., Fan, W., and Liu, Q. (2017). Circ100284, via miR-217 regulation of EZH2, is involved in the arsenite-accelerated cell cycle of human keratinocytes in carcinogenesis. Biochim. Biophys. Acta Mol. Basis Dis. *1863*, 753–763.

36. Tam, L.M., Price, N.E., and Wang, Y. (2020). Molecular mechanisms of arsenic-induced disruption of DNA repair. Chem. Res. Toxicol. *33*, 709–726.

37. Lai, Y., Zhao, W., Chen, C., Wu, M., and Zhang, Z. (2011). Role of DNA polymerase beta in the genotoxicity of arsenic. Environ. Mol. Mutagen. *52*, 460–468.

38. Litwin, I., Bocer, T., Dziadkowiec, D., and Wysocki, R. (2013). Oxidative stress and replication-independent DNA breakage induced by arsenic in Saccharomyces cerevisiae. PLoS Genet. *9*, e1003640.

39. Kong, Q., Deng, H., Li, C., Wang, X., Shimoda, Y., Tao, S., Kato, K., Zhang, J., Yamanaka, K., and An, Y. (2021). Sustained high expression of NRF2 and its target genes induces dysregulation of cellular proliferation and apoptosis is associated with arsenite-induced malignant transformation of human bronchial epithelial cells. Sci. Total Environ. *756*, 143840.

40. He, J., Wang, M., Jiang, Y., Chen, Q., Xu, S., Xu, Q., Jiang, B.H., and Liu, L.Z. (2014). Chronic arsenic exposure and angiogenesis in human bronchial epithelial cells via the ROS/miR-199a-5p/HIF-1alpha/COX-2 pathway. Environ. Health Perspect. *122*, 255–261.

41. Hamann, I., and Klotz, L.O. (2013). Arsenite-induced stress signaling: modulation of the phosphoinositide 3'-kinase/Akt/FoxO signaling cascade. Redox Biol. *1*, 104–109.

42. Liu, Y., Tang, J., Yuan, J., Yao, C., Hosoi, K., Han, Y., Yu, S., Wei, H., and Chen, G. (2020). Arsenite-induced downregulation of occludin in mouse lungs and BEAS-2B cells via the ROS/ERK/ELK1/MLCK and ROS/p38 MAPK signaling pathways. Toxicol. Lett. *332*, 146–154.

43. Yu, Z., Zhu, X., Li, Y., Liang, M., Liu, M., Liu, Z., Qin, L., Wu, X., Du, K., Liu, L., et al. (2021). Circ-HMGA2 (hsa_circ_0027446) promotes the metastasis and epithelial-mesenchymal transition of lung adenocarcinoma cells through the miR-1236-3p/ZEB1 axis. Cell Death Dis. *12*, 313.

44. Verduci, L., Tarcitano, E., Strano, S., Yarden, Y., and Blandino, G. (2021). CircRNAs: role in human diseases and potential use as biomarkers. Cell Death Dis. *12*, 468.

45. Shaulian, E., and Karin, M. (2001). AP-1 in cell proliferation and survival. Oncogene *20*, 2390–2400.

46. Angel, P., Hattori, K., Smeal, T., and Karin, M. (1988). The jun proto-oncogene is positively autoregulated by its product, Jun/AP-1. Cell *55*, 875–885.

47. Hoang, V.T., Nyswaner, K., Torres-Ayuso, P., and Brognard, J. (2020). The protein kinase MAP3K19 phosphorylates MAP2Ks and thereby activates ERK and JNK kinases and increases viability of KRAS-mutant lung cancer cells. J. Biol. Chem. *295*, 8470–8479.

48. Qiao, G.B., Wang, R.T., Wang, S.N., Tao, S.L., Tan, Q.Y., and Jin, H. (2021). GRP75-mediated upregulation of HMGA1 stimulates stage I lung adenocarcinoma progression by activating JNK/c-JUN signaling. Thorac. Cancer *12*, 1558–1569.

49. Tong, L., Yang, H., Xiong, W., Tang, G., Zu, X., and Qi, L. (2021). circ_100984-miR-432-3p axis regulated c-Jun/YBX-1/beta-catenin feedback loop promotes bladder cancer progression. Cancer Sci. *112*, 1429–1442.

50. Dang, C.V. (2012). MYC on the path to cancer. Cell *149*, 22–35.

51. Gabay, M., Li, Y., and Felsher, D.W. (2014). MYC activation is a hallmark of cancer initiation and maintenance. Cold Spring Harb. Perspect. Med. *4*, a014241.

52. Shen, S., Yao, T., Xu, Y., Zhang, D., Fan, S., and Ma, J. (2020). CircECE1 activates energy metabolism in osteosarcoma by stabilizing c-Myc. Mol. Cancer *19*, 151.

53. Cai, J., Chen, Z., Wang, J., Wang, J., Chen, X., Liang, L., Huang, M., Zhang, Z., and Zuo, X. (2019). circHECTD1 facilitates glutaminolysis to promote gastric cancer progression by targeting miR-1256 and activating beta-catenin/c-Myc signaling. Cell Death Dis. *10*, 576.

54. Sun, J., Zhang, H., Tao, D., Xie, F., Liu, F., Gu, C., Wang, M., Wang, L., Jiang, G., Wang, Z., and Xiao, X. (2019). CircCDYL inhibits the expression of C-MYC to suppress cell growth and migration in bladder cancer. Artif. Cells Nanomed. Biotechnol. *47*, 1349–1356.

55. Liu, L.H., Tian, Q.Q., Liu, J., Zhou, Y., and Yong, H. (2019). Upregulation of hsa_circ_0136666 contributes to breast cancer progression by sponging miR-1299 and targeting CDK6. J. Cell. Biochem. *120*, 12684–12693.

56. Luo, C.W., Hou, M.F., Huang, C.W., Wu, C.C., Ou-Yang, F., Li, Q.L., Wu, C.C., and Pan, M.R. (2020). The CDK6-c-Jun-Sp1-MMP-2 axis as a biomarker and therapeutic target for triple-negative breast cancer. Am. J. Cancer Res. *10*, 4325–4341.